Feeding Behavior Modifies Daily Rhythms in Autonomic Signaling and Core Body Temperature to Shape 24-hour Rhythms in Cardiac Electrophysiology

Makoto Ono[1], Don E. Burgess[1], Sidney R. Johnson[1], Claude S. Elayi[2], Karyn A. Esser[3], Tanya S. Seward[1], Carie R. Boychuk[4], Rebecca A. Stalcup[1], Abhilash Prabhat[1], Elizabeth A. Schroder[1,5*], Brian P. Delisle[1*]

[1]Department of Physiology, University of Kentucky, Lexington, KY, USA
[2]CHI Saint Joseph Hospital, Lexington, KY, USA
[3]University of Florida, Gainesville, FL, USA
[4]Dalton Cardiovascular Research Center, Department of Biomedical Sciences, University of Missouri, Columbia, MO, USA
[5]Department of Internal Medicine, University of Kentucky, Lexington, KY, USA

*Contributed equally to the study

Running Title: Feeding Shapes 24-hour Rhythms in Cardiac Ephys

Corresponding authors:

Elizabeth A. Schroder
Department of Internal Medicine
859-323-5571
eschr0@uky.edu
780 Rose Street, Medical Science Building, Rm: MN-512, Lexington, KY 40536-0298

Brian P. Delisle
(859) 323-2797
brian.delisle@uky.edu
741 S Limestone Street BBSRB B353, Lexington, KY, 40536

Word Count: 7,974

Key Words: Cardiac Electrophysiology**,** Time of Feeding**,** Core Temperature**,** Circadian Rhythms**,** Autonomic Nervous System

Abstract

Background: Circadian rhythms in physiology optimize organismal behavior to anticipate predictable environmental changes. Modern lifestyles can cause misalignment between ≈24-hour rhythms in feeding behavior from daily environmental cycles. Feeding behavior is a potent behavioral zeitgeber (timekeeping cue). We determined how shifting the timing of feeding behavior impacts the alignment of ≈24-hour rhythms in HR and cardiac electrophysiology in wild-type (WT) and *Scn5a*$^{+/\Delta KPQ}$ mice.

Methods: Mice eat most of their daily calories during the dark cycle. We shifted limited their food access to the light cycle (light-cycle restricted feeding or L-RF). Telemetry was used to continuously record changes in electrocardiogram (ECG), core body temperature (Tb), and activity. Cosinor and cross correlation analyses were used to analyze rhythmicity and 24-hour alignment between variables.

Results: L-RF for one day caused the 24-hour rhythms of the RR, QT, and PR intervals to shift 7-9 hours. The changes in the 24-hour ECG rhythms before and after the start of L-RF mirrored changes in daily body temperature (Tb) rhythm and correlated with changes in the high frequency (pHF) component of heart rate variability. Injecting mice undergoing L-RF with propranolol and atropine reduced the pHF component and caused a loss in the 24-hour rhythm in the RR interval and Tb. We identified a strong linear relation between the the QT interval and Tb. Normalizing the QT interval for Tb eliminated the 24-hour rhythm in the QT interval and identified abnormal changes in the QT interval in WT and *Scn5a*$^{+/\Delta KPQ}$ mice during L-RF.

Conclusion: Altering the timing of daily feeding behavior reshapes 24-hour rhythms in cardiac electrophysiology in mice by modifying daily rhythms in autonomic signaling and Tb. There is a strong linear relation between the QT interval and Tb. Normalizing the QT for Tb is important for identifying QT interval prolongation independent of Tb.

Abbreviations:

ALF - ad libitum fed
Electrocardiogram - ECG
L-RF - Light cycle restricted feeding
HR - Heart rate – (HR)
HRV – heart rate variability
MAP - Mean arterial pressure
pHF – high-frequency power
pLF – low-frequency power
Tb - core body temperature
SD- standard deviation
WT - Wild type
QT_{37^oC} – QT corrected to 37°C
ZT – Zeitgeber Time

Introduction

Modern lifestyles, including shift work and nighttime eating, disrupt evolutionarily conserved behavioral and environmental timekeeping cues critical for maintaining healthy circadian homeostatic mechanisms.[1] Disruption of these timekeeping cues and subsequent homeostasis is linked to an increased incidence of cardiovascular disease.[2,3] Understanding mechanistically how misaligned timekeeping cues ultimately impact cardiac function will provide new insight into how modern lifestyles can be improved to positively influence cardiac health and decrease arrhythmia susceptibility.

Daily rhythms of cardiac function usually align with daily feeding and activity cycles.[4] In mice, mean heart rate (HR) and mean arterial pressure (MAP) are highest during the dark cycle when mice are active and consume most of their daily calories.[5] Restricting food availability to the light cycle (light cycle-restricted feeding or L-RF) disrupts the alignment between daily feeding behavior and activity cycles. Importantly, L-RF in mice shifts the phase of the daily rhythms in HR and MAP (i.e., increases in HR and MAP) to align to the time of feeding and not activity, resulting in significantly higher HR and MAP during the light cycle compared to the dark cycle.[6,7] These data suggest that feeding behavior largely shapes the 24-hour rhythms in cardiovascular physiology. The purpose of this study is to determine the mechanism by which feeding behavior impacts the 24-hour rhythm of HR and cardiac electrophysiology.

Previous studies show that L-RF in mice shifts the phase and increases the amplitude of the daily core body temperature (Tb) rhythm.[8,9] Several studies show that HR increases and decreases with Tb.[10-14] We tested the idea that the L-RF induced change in the daily Tb rhythm facilitates drives the realignment of the daily rhythms in HR and cardiac electrophysiology to feeding behavior.

Methods

Animals. All the mice used in this study were male SV129 mice. Wild type (WT) and *Scn5a*$^{+/\Delta KPQ}$ mice used in longitudinal L-RF studies were 3-4 months old, and mice used for pharmacological studies were 6-8 months old. All procedures complied with the Association for Assessment and Accreditation of Laboratory Animal Care guidelines and were approved by the Institutional Animal Care and Use Committee at the University of Kentucky. Dr. Peter Carmeliet kindly provided the *Scn5a*$^{+/\Delta KPQ}$ mouse strain.[15] This study represents new and reanalysis of data collected previously.[6]

Light Cycle Restricted Feeding. Mice were housed in 12-hour light/dark cycles at room temperature with ad libitum access to water. To initiate L-RF, food was removed at 9 h after the beginning of the light cycle (Zeitgeber time or ZT = 9). The next day, food presentation was restricted for 7 h during the light cycle, between ZT 2–9 for up to two weeks unless otherwise noted. L-RF caused mice to lose body mass during the first week (**Figure S1**). However, caloric intake increased after that, and L-RF animals gained body mass after two weeks.[16] Telemetry recordings were performed in ad libitum fed conditions (ALF) before L-RF, shortly after starting L-RF, and two weeks after the start of L-RF.

ECG, Tb, and Locomotor Activity Measurements by Telemetry. We used telemetry to measure electrocardiogram (ECG), Tb, and locomotor activity. Mice were anesthetized

with isoflurane and implanted with PhysioTel ETA-F10 (Data Sciences International) telemetry transmitter units. ECG telemetry data were recorded at 1000 Hz, and RR and QT interval analyses were done using MATLAB (MathWorks), similar to previously described.[6,17,18] ECG traces recorded for each hour were aligned to the peak of the R wave to generate an averaged ECG trace. The start of the P wave was defined as the point where the slope of the P wave profile changed by more than 0.001 mV/ms; the Q wave was defined as the point where the slope of the profile changed from negative to positive at the base of the QRS complex; the end of the T wave was defined as the point of intersection of T wave maximum slope with baseline.[19]

The hourly mean data for RR, QT, and PR intervals and Tb were fit with the cosine curve function:

$$\text{Interval} = A*\cos[2\pi*t/T - \emptyset] + m$$

to calculate the period (T), the time between the peak amplitudes; acrophase (∅), the phase of the peak amplitude in relation to the start of the light cycle (ZT = 0); the amplitude (A), one-half of the peak to trough amplitude; and the mesor (m), the rhythm adjusted mean.[6,17,18]

Heart rate variability (HRV) was calculated as outlined previously.[20] RR interval time series were generated for R wave peak detection. The frequency range used to classify low frequency was 0.4-1.5 Hz, and the frequency range to classify high frequency was 1.5-4.0 Hz.[20]

We used cross-correlation between time series to compare the rhythmicity and phase alignment of the RR interval and Tb, the strength of the high frequency (pHF) HRV component, or activity.[21] The RR interval time series was lagged against the time series for the Tb, pHF component, or activity. If the time series are in phase, the peak cross-correlation will occur at lag 0. A regular rise and fall in the cross-correlation between variables with a lag of 0 indicates correlated rhythmicity between the different time series. We used the R function “ccf” to calculate the cross-correlation between two data sets.[22] The formula used in “ccf” to calculate the cross-correlation between two time series $X(t), Y(t)$ has the form

$$c_{xy}(t) = \frac{1}{n} \sum_{s=\max(1,-t)}^{\min(n-t,n)} [X(s+t) - \bar{X}]\,[Y(s+t) - \bar{Y}]\,,\; r_{xy}(t) = \frac{c_{xy}(t)}{c_{xy}(0)}$$

This study also corrected the hourly mean in the QT interval for Tb. We used an approach similar to that described previously to generate the Tb correction formula.[23] The hourly mean QT intervals were plotted against the corresponding Tb for all data collected in ALF, after the start of L-RF, and two weeks after the start of L-RF. The data were described using linear regression, and the R^2 for a linear relationship was significant for each data set. The average slope of the linear QT-Tb relation was used to derive the correction formula. We corrected the QT intervals to 37°C ($QT_{37°C}$ interval) because 37°C was the daily mean in the Tb for mice in ALF.

$$QT_{37°C} = \text{QT interval} - (4.3*(37°C - Tb))$$

We demonstrated that the QT_{37^oC} interval generated a horizontal line in the corrected QT_{37^oC} -Tb plots to validate the formula.

Propranolol and atropine injections. We assessed the effect of L-RF on RR interval following intraperitoneal (IP) injection of propranolol hydrochloride and atropine sulfate (propranolol and atropine; 10 mg/kg each) to block β-adrenergic and muscarinic receptors, respectively, similar to that previously reported.[24-26] We did longitudinal studies and injected telemetered mice undergoing L-RF at ZT 23.5 (when the daily rhythm in the RR interval peaked) and 9.5 (when the RR interval was at its nadir) for two consecutive days. The L-RF protocol for these mice was to provide food access between ZT 3 and ZT 9. Feeding onset was delayed one hour to separate the food anticipatory decrease in RR interval before feeding from the start of the light cycle.

Statistical analysis. For some graphs, data are shown as the mean and standard deviation of the mean (SD). For other graphs, a data point for each animal is shown with a horizontal bar at the mean. The statistical JTK_CYCLE package was used to confirm statistically significant cyclical rhythms before analyzing the data using cosine waveform curve fitting.[27] Data were analyzed in PRISM (GraphPad). Data between two groups were analyzed using a T-test, and data sets with more than two groups were analyzed using a 1-way or 2-way ANOVA. Post-hoc testing was done using Šidák. $p<0.05$ was considered significant.

Results

L-RF simultaneously modifies 24-hour rhythms in HR, cardiac electrophysiology, and Tb.

This study aimed to identify the mechanism(s) for the impact of L-RF in mice on daily rhythms in HR (as measured by the RR interval) and cardiac electrophysiology. We used *in vivo* telemetry to longitudinally record ECG data from mice in ALF, after the initial start of L-RF, and two weeks after the start of L-RF (**Figure 1A**). Data recorded shortly after starting L-RF revealed the acute impact L-RF had on cardiac electrophysiology, and data recorded two weeks after starting L-RF indicated steady-state (i.e., chronic) changes L-RF had on cardiac electrophysiology.[9] The top panel in **Figure 1B** shows a three-day time series for changes in the hourly mean in the RR interval, the duration of ventricular repolarization (the QT interval), and the duration of atrial to ventricular conduction (the PR interval). All three of the time series for the hourly mean of the RR, QT, and PR intervals displayed daily rhythms that aligned with each other and peaked at a similar time during the light cycle (unshaded areas). However, one day after starting L-RF, the daily rhythms in ECG data exhibited large simultaneous shifts in phase, resulting in peaks (i.e., longer wave durations and slower HRs) during the dark cycle. These 'dark cycle' peaks were also notably larger in amplitude than before L-RF started. These changes were not transitory and persisted throughout L-RF (i.e., two weeks after the start of L-RF).

L-RF causes similar causes similar shifts in daily Tb rhythms.[9,28] We tested whether L-RF-induced changes in Tb rhythm (i.e., robust drops in Tb during the dark cycle) occurred simultaneously with the changes in the ECG. We compared the hourly mean in Tb for the same days as ECG data from mice in ALF, after starting L-RF, and two

weeks after starting L-RF (**Figure 1B**). The daily Tb rhythm mirrored daily rhythms in RR, QT, and PR intervals before and after the start of L-RF.

The individual ECG and Tb time series recorded from mice in ALF, one day after starting L-RF, and two weeks after starting L-RF were significant cyclical rhythms well described using cosine curve fitting. We used cosine curve fitting to the individual mouse data to calculate the phase shifts caused by L-RF (**Figures 1B and 2A**). Data showed that the acrophase of the daily rhythms in the RR intervals, QT intervals, PR intervals, and Tb shifted 7-9 hours shortly after starting L-RF. Only small additional changes were seen after two weeks in L-RF. Although L-RF caused abrupt changes in the phase of the ECG and Tb data, the periodicity of the daily ECG and Tb rhythms remained ≈24 hours (**Figure 2A**).

Cosine curve fitting allowed us to calculate the impact that L-RF had on the mesor and amplitude of the 24-hour rhythms in RR intervals, QT intervals, PR intervals, and Tb (**Figure 2B**). Compared to data recorded in ALF, the mesor and amplitudes of 24-hour rhythms in RR and QT intervals increased one day after starting L-RF and persisted as long as recorded (two weeks after starting L-RF). Analogous changes were seen in the mesor and amplitude of the Tb rhythm. In contrast, the L-RF-induced changes in the 24-hour rhythm of the PR interval did not occur immediately. Alterations in mesor and amplitude of the PR interval were only detected two weeks after starting L-RF.

L-RF-induced changes in the RR interval correlate with changes in HRV but not activity

The 24-hour rhythm in the RR interval is classically thought to reflect changes in efferent signaling from the autonomic nervous system (ANS), endocrine system, and daily activity cycles.[29-31] We quantified changes in ANS cardiac regulation by measuring HRV in the frequency domain.[20] We focused on the pHF component as an index for parasympathetic motor efferent regulation of cardiac function since L-RF caused an overall slowing of HR. For mice in ALF, the amplitude of the pHF component was higher during the light cycle compared to the dark cycle. One day after starting L-RF, the pHF component increased during the dark cycle (**Figure 1B**), and the increase persisted two weeks after starting L-RF.

We also measured the time series in activity from the mice in ALF, after starting L-RF, and two weeks after starting L-RF (**Figure 1B**). In ALF mice, mouse activity is highest during the dark cycle. However, the activity peaks during the dark cycle were less apparent after starting L-RF because activity profiles showed multiple peaks during the light and dark cycles.

The individual mouse three-day time series data for the pHF component and activity rhythms did not show robust significant cyclical rhythms, and they were not well described by cosine waveform curve fitting. Therefore, we analyzed the relative rhythmicity between the RR interval and pHF or activity using cross-correlation analyses.[21] As part of the analysis, we included the cross-correlation between RR-Tb. **Figure 3** shows the cross-correlation results for the RR-Tb, RR-pHF, and RR-activity from mice in ALF, one day after starting L-RF, and two weeks after starting L-RF. The RR-Tb and RR-pHF showed correlated rhythmicity that peaked with a lag of 0. A qualitatively similar correlated rhythmicity was seen in the cross-correlation for RR-

activity during ALF, but the correlated rhythmicity was lost after starting L-RF. The data suggest Tb and autonomic signaling may be important for shaping the daily rhythm in the RR interval recorded from mice in L-RF.

Propranolol and atropine cause a loss in daily RR interval and Tb rhythms during L-RF

We determined how propranolol and atropine injections impacted the 24-hour rhythm in mean RR interval and Tb from mice in L-RF (fed from ZT 3 to 9). Mice were subjected to L-RF for one week and then injected with propranolol and atropine at ZT 23.5 (**Figure 4A**). We confirmed that propranolol and atropine injection reduced the amplitude of the pHF and pLF components (**Figure 4B)**. We found that the injection only caused minor changes in the mean RR interval and Tb when compared to the same time on the previous day (**Figure 2S, Figure 4A,** and **Figure 4B**). Repeating the propranolol and atropine injection at ZT 9.5 also caused only small changes in the mean RR interval and Tb compared to the same time on the previous day (**Figure 2S and 4A**). However, several hours after the injection at ZT 9.5, the RR interval did not increase and Tb did not decrease during the dark cycle (**Figure 4C**). Repeating the injections of propranolol and atropine at ZT 23.5 and 9.5 for a second day also prevented the increase in the RR interval and the decrease in Tb during the subsequent dark cycle. The data demonstrate that injecting mice in L-RF with propranolol and atropine resulted in a loss in the daily rhythm of the RR interval and Tb in L-RF mice (**Figure 4C**). We conclude that, during L-RF, the daily rhythm in the RR interval is strongly linked to changes in the autonomic signaling and the daily Tb rhythm.

L-RF reveals a robust linear QT-Tb relation in WT mice

The time series data show that longitudinal changes in the mean QT interval are similar to the RR interval and mirror the Tb rhythm (**Figure 1**). Previous studies demonstrate that QT interval duration in mice is independent of RR interval.[32-35] Therefore, we quantified the linear relation between the hourly QT interval and Tb using data recorded from mice in ALF, initially after starting L-RF, and two weeks after starting L-RF similar to that described for beagles (**Figure 5A**).[23] We found a strong negative linear relationship, and we used the average slope of linear regression analyses to normalize the QT interval data to a mean Tb of ALF (37ºC) (**Figure 5A**). Normalizing the time series of the QT interval for a Tb of 37ºC caused a loss in the 24-hour rhythm in the QT interval for mice in ALF and L-RF (**Figure 5B**).

Correcting the QT interval unmasks differences in the QT interval between WT and $Scn5a^{+/\Delta KPQ}$ mice

To determine the physiological significance for the QT interval dependence on Tb we studied a transgenic mouse model of long QT type 3 syndrome ($Scn5a^{+/\Delta KPQ}$) before and after L-RF similar to that described for WT mice in **Figure 1**. We measured ECG properties and Tb in ALF, immediately after starting L-RF, and two weeks after starting L-RF. The changes in the daily rhythms of the ECG and Tb data after starting L-RF were qualitatively and quantitatively similar to those recorded in WT mice (**Figure 6A, 6B, Figure 3S**). Cosine fitting analysis of ECG data from the $Scn5a^{+/\Delta KPQ}$ mice showed that one day after starting L-RF, there was an immediate shift in the phase for RR, QT, and PR intervals and Tb, an increase in the amplitudes of the rhythms, an increase in

213 the mesor of the RR, QT, and PR intervals, and a decrease in the mesor for Tb (**Figure**
214 **3S**). There were some genotype-specific differences in the mesor and amplitude for RR
215 intervals, QT intervals, and Tb between the WT and *Scn5a*$^{+/\Delta KPQ}$ mice. We calculated
216 the QT_{37^oC} interval for *Scn5a*$^{+/\Delta KPQ}$ mice in ALF, after starting L-RF, and two weeks after
217 starting L-RF, and we compared the the QT_{37^oC} interval data form the *Scn5a*$^{+/\Delta KPQ}$ mice
218 with WT mice (**Figure 6B**). The QT_{37^oC} interval was not different between WT and
219 *Scn5a*$^{+/\Delta KPQ}$ mice in ALF. However, after starting L-RF, the QT_{37^oC} interval measured in
220 *Scn5a*$^{+/\Delta KPQ}$ mice became longer than the QT_{37^oC} interval measured from WT mice
221 (**Figure 3S**). We also identified a genotype-specific difference in how L-RF impacted the
222 QT_{37^oC} interval in WT and *Scn5a*$^{+/\Delta KPQ}$ mice. In WT mice, L-RF increased the QT_{37^oC}
223 interval only after two weeks, but in *Scn5a*$^{+/\Delta KPQ}$ mice, the QT_{37^oC} interval increased only
224 after one day (**Figure 3S**).

225 **Discussion**

226 In this study, we demonstrate that one day after starting L-RF, 24-hour rhythms in
227 mean RR, QT, and PR intervals and Tb shifted simultaneously by 7-9 hours to a new
228 phase and remained at this new phase for the duration of L-RF. The 24-hour rhythms in
229 L-RF were shaped by increased ECG interval durations and lower Tb measured during
230 the dark cycles. The increase of the RR interval correlated with the changes in the
231 amplitude of the pHF component in HRV analysis and did not depend on the activity.
232 Repeated inhibition of *β*-adrenergic and muscarinic receptors in mice undergoing L-RF
233 prevented the increase in RR interval and decrease in Tb during the dark cycle-
234 resulting in the loss of the daily RR interval and Tb rhythms in mice during L-RF. We
235 also identified a strong linear relation between the hourly mean in the QT interval and
236 Tb. Correcting the QT interval for Tb allowed us to identify abnormal changes in the QT
237 interval measured from WT and *Scn5a*$^{+/\Delta KPQ}$ mice independent of Tb.

238 Studies suggested that the circadian clock in the suprachiasmatic nucleus (SCN)
239 modified ANS signaling to generate the 24-hour rhythm in HR.[4,30,36-38] These studies
240 were supported by data showing that ablation of SCN or transgenic mice lacking the
241 core circadian clock transcription factor *Bmal1* (e.g., *Bmal1*$^{-/-}$) did not have a 24-hour
242 rhythm in HR.[39-41] L-RF is not thought to impact the circadian clock mechanism in the
243 SCN;[9] therefore, it was surprising that our previous work demonstrated that L-RF
244 caused a large phase shift in the 24-hour rhythm of the HR.[6] L-RF in mice also shifts the
245 phase of circadian gene expression in peripheral tissues, including the heart, to align
246 with the timing of feeding behavior.[9] Several studies implicate the cardiomyocyte
247 circadian clock in regulating gene expression essential for cardiac excitability, cardiac
248 electrophysiology, and HR.[18,35,40,42-45] One might predict then that L-RF shifts the phase
249 of cardiomyocyte gene expression to facilitate the phase shift in HR and cardiac
250 electrophysiology. However, genetically disrupting the cardiomyocyte-specific circadian
251 clock (by inducing the deletion of *Bmal1*) does not abolish the L-RF mediated phase
252 shift in the daily HR and cardiac electrophysiological rhythms.[17] Additionally, we tested
253 for a difference in the HR measured from mice in ALF vs. L-RF after injecting
254 propranolol and atropine (**Figure 5S**). We did not detect a difference in HR between
255 these two groups after injection. Together, the data demonstrate that the observed
256 changes in HR with L-RF are not secondary to changes in cardiomyocyte circadian

clock signaling or intrinsic to the heart. The changes in HR with L-RF appear to be secondary to daily changes in autonomic signaling and Tb.

The QT interval is used clinically to assess people's risk for deadly ventricular arrhythmias.[46] In humans, the QT interval changes as a function of the RR interval, and several formulas can correct the QT interval for HR. Although HR correction formulas for the QT interval in mice exist,[47] the most commonly used correction formula was derived by measuring the average HR and corresponding QT interval across the 24-hour cycle. The temperature dependence of the QT interval and daily rhythm in Tb were not considered. Importantly, recent studies show mice have a weak HR adaptation of the QT interval[32,33,48] and applying the QT interval correction leads to overcorrection and errors. We suspected that the daily rhythm in the QT interval used to derive the QT interval correction in mice may have reflected daily rhythms in Tb and not HR. Consistent with this idea, we now report a robust linear QT-Tb relation in mice, and correcting the QT interval for Tb caused a loss in the daily rhythm of the QT interval in mice during ALF and L-RF. These new data raise the possibility that the daily rhythm in the QT interval in mice primarily reflects Tb. This possibility is also supported by a study showing the 24-hours rhythm of the QT interval in mice is independent of the daily RR rhythm.[35] Tb was not measured in this study, but the observed change in the amplitude of the daily rhythm in the QT interval (4-5 ms) is consistent with an expected amplitude change of the daily Tb rhythm in mice (1°C).[49]

We extended our L-RF studies to quantify the changes in the QT interval in a transgenic knock-in mouse model that expresses a mutation linked to long QT syndrome in people.[15] Correcting the QT interval for Tb allowed direct comparisons of QT intervals at different Tb across the 24-hour cycle, identified genotype-specific differences in the QT interval independent of Tb, and showed that L-RF caused a prolongation of the QT interval in *Scn5a*$^{+/\Delta KPQ}$ mice (but not WT mice) after only one day. These results are qualitatively different if the QT interval is not corrected for Tb and underscore the importance of monitoring and considering the impact of Tb when measuring ECGs in mice.

Implications

Modern lifestyles disrupt evolutionarily conserved behavioral and environmental timekeeping cues critical for maintaining healthy circadian homeostatic mechanisms.[1] We found that a misalignment of the timing of feeding behavior relative to the light/dark cycle causes dramatic changes in the daily rhythms of HR and cardiac electrophysiology in mice. These changes appeared to be driven by changes in ANS signaling and Tb. Our findings suggest feeding behavior is a critical timekeeping cue for the daily Tb and cardiac electrophysiology rhythms in mice. If conserved, modern lifestyles that disrupt evolutionary conserved feeding rhythms in people may negatively impact the alignment between daily circadian and cardiac electrophysiological to impair cardiac performance and influence arrhythmogenic risk.

Another implication of this study is that it underscores the importance that daily rhythms in Tb have in shaping 24-hour rhythms in cardiac electrophysiology. Continuous monitoring of Tb is not routinely performed in people undergoing electrophysiological testing despite representing an important contributor to the HR and

301 QTc intervals. This is especially true in studies that monitor changes in HR and QTc
302 interval across the 24-hour cycle. Several studies estimate that the Q10 in the HR of
303 mice is between 2-2.5.[13,14] The Q10 in HR reflect a conserved structural and functional
304 property of HCN channels that directly couples temperature to cell membrane
305 excitability.[14] A HR with a Q10 of 2-2.5 predicts that 50-75% of the observed amplitude
306 in the daily rhythm of the RR interval is secondary to the daily rhythm Tb. Our data
307 suggest Tb is also important for shaping the 24-hour rhythm in the QT interval in mice.
308 Based on previously published data, we propose that the daily rhythm in Tb also
309 contributes to the 24-hour rhythm in the QTc interval observed in people. Several
310 studies report a temperature dependence of the QTc interval in people as 10-15 ms for
311 every 1°C change.[23,50-54] The peak to trough amplitude in the daily Tb rhythm in people
312 is about 1°C, and the peak to trough amplitude in the daily rhythm in the QTc is 10-20
313 ms.[55,56] Future studies that measure both ECG parameters and Tb across the 24-hour
314 cycle in people will help to delineate how much of the 24-hour rhythms in cardiac
315 electrophysiology are due to daily rhythms in Tb. Importantly, measuring the Tb and the
316 QTc interval together may help to delineate abnormal changes in the QT interval
317 secondary to repolarization abnormalities vs. abnormal changes in Tb.

318 *Limitations*

319 These studies were performed in mice at room temperature, and mice housed at
320 room temperature are vulnerable to torpor during fasting. Torpor is a transient
321 hibernating-like state that causes a large drop in Tb (below 32°C) and slow HR.[13] Our
322 model of L-RF did not calorically restrict the mice. The mice continued to eat 3-4 grams
323 of food per day during L-RF (**Figure 1S**), gained mass after one week in L-RF (**Figure**
324 **1S**), and Tb analysis showed only one mouse briefly had a Tb < 33°C after starting L-
325 RF (**Figure 4S**). Another limitation this study used only male mice. We chose male mice
326 because female mice are more prone to bouts of torpor.[13] It also remains unclear
327 whether a longer $QT_{37°C}$ interval is associated with an increased risk for spontaneous
328 ventricular arrhythmias. The lack of spontaneous arrhythmias in *Scn5a*$^{+/\Delta KPQ}$ mice is not
329 surprising because the absolute incidence of spontaneous arrhythmias in these mice
330 and people with LQT3 is extremely low. We found that, during L-RF, the daily rhythm in
331 the PR interval simultaneously shifted with the RR and QT intervals and Tb. However,
332 due to the small amplitude and relatively slow change in the PR interval in response to
333 L-RF, it was difficult to determine if Tb contributed to changes in the PR interval. Lastly,
334 caution must be used when extrapolating ECG data obtained from mice to people.[34,57]

335 *Summary*

336 Daily rhythms in HR and cardiac electrophysiology align with feeding and activity
337 cycles via signals originating from the SCN. However, when food availability becomes
338 restricted to the light cycle, this disrupts the association between environmental and
339 behavioral timekeeping cues, and daily rhythms in HR and cardiac electrophysiology
340 align with the new feeding behavior and Tb. We conclude that L-RF-induced changes in
341 the daily autonomic signaling and Tb rhythms are important for facilitating the
342 realignment 24-hour rhythms in HR and cardiac electrophysiology, and the daily
343 variation in the Tb rhythm helps to shape the daily rhythms in the RR and QT intervals.

344

Competing interests

None declared.

Author contributions

All authors contributed to drafting the work and revising it critically for important intellectual content, approved the final version of the manuscript, and qualified for authorship.

Funding

This work was supported by National Heart Lung and Blood Institute grants R01HL153042 and R01HL141343.

Acknowledgement

We would like to thank Drs. Wayne Giles and Chao-Yin Chen (University of California, Davis) for providing feedback and discussion. We would also like to acknowledge Isabel Stumpf (Centre College) and David Schneider (Centre College) for technical assistance.

References

1. Gohari A, Wiebe D, Ayas N. Shift working and cardiovascular health. *Chronobiol Int*. 2023;40:27-32. doi: 10.1080/07420528.2021.1933000
2. Yang L, Luo Y, He L, Yin J, Li T, Liu S, Li D, Cheng X, Bai Y. Shift Work and the Risk of Cardiometabolic Multimorbidity Among Patients With Hypertension: A Prospective Cohort Study of UK Biobank. *J Am Heart Assoc*. 2022;11:e025936. doi: 10.1161/JAHA.122.025936
3. Xu C, Weng Z, Liang J, Liu Q, Zhang X, Xu J, Li Q, Zhou Y, Gu A. Shift Work, Genetic Factors, and the Risk of Heart Failure: A Prospective Study of the UK Biobank. *Mayo Clin Proc*. 2022;97:1134-1144. doi: 10.1016/j.mayocp.2021.12.003
4. Schroder EA, Delisle BP. Time Restricted Feeding to the Light Cycle Dissociates Canonical Circadian Clocks and Physiological Rhythms in Heart Rate. *Front Pharmacol*. 2022;13:910195. doi: 10.3389/fphar.2022.910195
5. Li P, Sur SH, Mistlberger RE, Morris M. Circadian blood pressure and heart rate rhythms in mice. *Am J Physiol*. 1999;276:R500-504. doi: 10.1152/ajpregu.1999.276.2.R500
6. Schroder EA, Burgess DE, Manning CL, Zhao Y, Moss AJ, Patwardhan A, Elayi CS, Esser KA, Delisle BP. Light phase-restricted feeding slows basal heart rate to exaggerate the type-3 long QT syndrome phenotype in mice. *Am J Physiol Heart Circ Physiol*. 2014;307:H1777-1785. doi: 10.1152/ajpheart.00341.2014
7. Zhang D, Colson JC, Jin C, Becker BK, Rhoads MK, Pati P, Neder TH, King MA, Valcin JA, Tao B, et al. Timing of Food Intake Drives the Circadian Rhythm of Blood Pressure. *Function (Oxf)*. 2021;2:zqaa034. doi: 10.1093/function/zqaa034
8. Schibler U, Gotic I, Saini C, Gos P, Curie T, Emmenegger Y, Sinturel F, Gosselin P, Gerber A, Fleury-Olela F, et al. Clock-Talk: Interactions between Central and Peripheral Circadian Oscillators in Mammals. *Cold Spring Harb Symp Quant Biol*. 2015;80:223-232. doi: 10.1101/sqb.2015.80.027490
9. Damiola F, Le Minh N, Preitner N, Kornmann B, Fleury-Olela F, Schibler U. Restricted feeding uncouples circadian oscillators in peripheral tissues from the central pacemaker in the suprachiasmatic nucleus. *Genes Dev*. 2000;14:2950-2961. doi: 10.1101/gad.183500
10. Clark AJ. The effect of alterations of temperature upon the functions of the isolated heart. *J Physiol*. 1920;54:275-286. doi: 10.1113/jphysiol.1920.sp001929
11. Tanner JM. The relationships between the frequency of the heart, oral temperature and rectal temperature in man at rest. *J Physiol*. 1951;115:391-409. doi: 10.1113/jphysiol.1951.sp004677
12. Kirschen GW, Singer DD, Thode HC, Jr., Singer AJ. Relationship between body temperature and heart rate in adults and children: A local and national study. *Am J Emerg Med*. 2020;38:929-933. doi: 10.1016/j.ajem.2019.158355
13. Swoap SJ, Gutilla MJ. Cardiovascular changes during daily torpor in the laboratory mouse. *Am J Physiol Regul Integr Comp Physiol*. 2009;297:R769-774. doi: 10.1152/ajpregu.00131.2009

14. Wu Y, Wang Q, Granger J, Gaido OR, Aguilar EN, Ludwig A, Moroni A, Bianchet MA, Anderson ME. HCN channels sense temperature and determine heart rate responses to heat. *bioRxiv*. 2023. doi: 10.1101/2023.09.02.556046
15. Nuyens D, Stengl M, Dugarmaa S, Rossenbacker T, Compernolle V, Rudy Y, Smits JF, Flameng W, Clancy CE, Moons L, et al. Abrupt rate accelerations or premature beats cause life-threatening arrhythmias in mice with long-QT3 syndrome. *Nature Medicine*. 2001;7:1021-1027. doi: 10.1038/nm0901-1021
16. Bray MS, Ratcliffe WF, Grenett MH, Brewer RA, Gamble KL, Young ME. Quantitative analysis of light-phase restricted feeding reveals metabolic dyssynchrony in mice. *Int J Obes (Lond)*. 2013;37:843-852. doi: 10.1038/ijo.2012.137
17. Schroder EA, Burgess DE, Johnson SR, Ono M, Seward T, Elayi CS, Esser KA, Delisle BP. Timing of food intake in mice unmasks a role for the cardiomyocyte circadian clock mechanism in limiting QT-interval prolongation. *Chronobiol Int*. 2021:1-10. doi: 10.1080/07420528.2021.2011307
18. Schroder EA, Burgess DE, Zhang X, Lefta M, Smith JL, Patwardhan A, Bartos DC, Elayi CS, Esser KA, Delisle BP. The cardiomyocyte molecular clock regulates the circadian expression of Kcnh2 and contributes to ventricular repolarization. *Heart Rhythm*. 2015;12:1306-1314. doi: 10.1016/j.hrthm.2015.02.019
19. Lund K, Nygaard H, Kirstein Pedersen A. Weighing the QT intervals with the slope or the amplitude of the T wave. *Ann Noninvasive Electrocardiol*. 2002;7:4-9. doi: 10.1111/j.1542-474x.2001.tb00132.x
20. Fenske S, Probstle R, Auer F, Hassan S, Marks V, Pauza DH, Biel M, Wahl-Schott C. Comprehensive multilevel in vivo and in vitro analysis of heart rate fluctuations in mice by ECG telemetry and electrophysiology. *Nat Protoc*. 2016;11:61-86. doi: 10.1038/nprot.2015.139
21. Levine JD, Funes P, Dowse HB, Hall JC. Signal analysis of behavioral and molecular cycles. *BMC Neurosci*. 2002;3:1. doi: 10.1186/1471-2202-3-1
22. Team Rc. R: A Language and Environment for Statistical Computing. R Foundation for Statistical Computing. https://www.R-project.org. 2020.
23. van der Linde HJ, Van Deuren B, Teisman A, Towart R, Gallacher DJ. The effect of changes in core body temperature on the QT interval in beagle dogs: a previously ignored phenomenon, with a method for correction. *Br J Pharmacol*. 2008;154:1474-1481. doi: 10.1038/bjp.2008.265
24. Rose RA, Kabir MG, Backx PH. Altered heart rate and sinoatrial node function in mice lacking the cAMP regulator phosphoinositide 3-kinase-gamma. *Circ Res*. 2007;101:1274-1282. doi: 10.1161/CIRCRESAHA.107.158428
25. Krishnaswamy PS, Egom EE, Moghtadaei M, Jansen HJ, Azer J, Bogachev O, Mackasey M, Robbins C, Rose RA. Altered parasympathetic nervous system regulation of the sinoatrial node in Akita diabetic mice. *J Mol Cell Cardiol*. 2015;82:125-135. doi: 10.1016/j.yjmcc.2015.02.024
26. Egom EE, Vella K, Hua R, Jansen HJ, Moghtadaei M, Polina I, Bogachev O, Hurnik R, Mackasey M, Rafferty S, et al. Impaired sinoatrial node function and increased susceptibility to atrial fibrillation in mice lacking natriuretic peptide receptor C. *J Physiol*. 2015;593:1127-1146. doi: 10.1113/jphysiol.2014.283135

27. Hughes ME, Hogenesch JB, Kornacker K. JTK_CYCLE: an efficient nonparametric algorithm for detecting rhythmic components in genome-scale data sets. *J Biol Rhythms*. 2010;25:372-380. doi: 10.1177/0748730410379711
28. Satoh Y, Kawai H, Kudo N, Kawashima Y, Mitsumoto A. Time-restricted feeding entrains daily rhythms of energy metabolism in mice. *Am J Physiol Regul Integr Comp Physiol*. 2006;290:R1276-1283. doi: 10.1152/ajpregu.00775.2005
29. Barazi N, Polidovitch N, Debi R, Yakobov S, Lakin R, Backx PH. Dissecting the Roles of the Autonomic Nervous System and Physical Activity on Circadian Heart Rate Fluctuations in Mice. *Front Physiol*. 2021;12:692247. doi: 10.3389/fphys.2021.692247
30. Tong M, Watanabe E, Yamamoto N, Nagahata-Ishiguro M, Maemura K, Takeda N, Nagai R, Ozaki Y. Circadian expressions of cardiac ion channel genes in mouse might be associated with the central clock in the SCN but not the peripheral clock in the heart. *Biol Rhythm Res*. 2013;44:519-530. doi: 10.1080/09291016.2012.704801
31. Gordan R, Gwathmey JK, Xie LH. Autonomic and endocrine control of cardiovascular function. *World J Cardiol*. 2015;7:204-214. doi: 10.4330/wjc.v7.i4.204
32. Mulla W, Murninkas M, Levi O, Etzion Y. Incorrectly corrected? QT interval analysis in rats and mice. *Front Physiol*. 2022;13:1002203. doi: 10.3389/fphys.2022.1002203
33. Mulla W, Gillis R, Murninkas M, Klapper-Goldstein H, Gabay H, Mor M, Elyagon S, Liel-Cohen N, Bernus O, Etzion Y. Unanesthetized Rodents Demonstrate Insensitivity of QT Interval and Ventricular Refractory Period to Pacing Cycle Length. *Front Physiol*. 2018;9:897. doi: 10.3389/fphys.2018.00897
34. Ripplinger CM, Glukhov AV, Kay MW, Boukens BJ, Chiamvimonvat N, Delisle BP, Fabritz L, Hund TJ, Knollmann BC, Li N, et al. Guidelines for assessment of cardiac electrophysiology and arrhythmias in small animals. *Am J Physiol Heart Circ Physiol*. 2022;323:H1137-H1166. doi: 10.1152/ajpheart.00439.2022
35. Gottlieb LA, Larsen K, Halade GV, Young ME, Thomsen MB. Prolonged QT intervals in mice with cardiomyocyte-specific deficiency of the molecular clock. *Acta Physiol (Oxf)*. 2021;233:e13707. doi: 10.1111/apha.13707
36. Scheer FA, Hilton MF, Mantzoros CS, Shea SA. Adverse metabolic and cardiovascular consequences of circadian misalignment. *Proc Natl Acad Sci U S A*. 2009;106:4453-4458. doi: 10.1073/pnas.0808180106
37. Sano H, Hayashi H, Makino M, Takezawa H, Hirai M, Saito H, Ebihara S. Effects of suprachiasmatic lesions on circadian rhythms of blood pressure, heart rate and locomotor activity in the rat. *Jpn Circ J*. 1995;59:565-573. doi: 10.1253/jcj.59.565
38. Warren WS, Champney TH, Cassone VM. The suprachiasmatic nucleus controls the circadian rhythm of heart rate via the sympathetic nervous system. *Physiol Behav*. 1994;55:1091-1099. doi: 10.1016/0031-9384(94)90392-1
39. Curtis AM, Cheng Y, Kapoor S, Reilly D, Price TS, Fitzgerald GA. Circadian variation of blood pressure and the vascular response to asynchronous stress. *Proc Natl Acad Sci U S A*. 2007;104:3450-3455. doi: 10.1073/pnas.0611680104

496 40. Schroder EA, Ono M, Johnson SR, Rozmus ER, Burgess DE, Esser KA, Delisle
497 BP. The role of the cardiomyocyte circadian clocks in ion channel regulation and
498 cardiac electrophysiology. *J Physiol*. 2022;600:2037-2048. doi:
499 10.1113/JP282402
500 41. Yang G, Chen L, Grant GR, Paschos G, Song WL, Musiek ES, Lee V,
501 McLoughlin SC, Grosser T, Cotsarelis G, et al. Timing of expression of the core
502 clock gene Bmal1 influences its effects on aging and survival. *Sci Transl Med*.
503 2016;8:324ra316. doi: 10.1126/scitranslmed.aad3305
504 42. Delisle BP, Stumpf JL, Wayland JL, Johnson SR, Ono M, Hall D, Burgess DE,
505 Schroder EA. Circadian clocks regulate cardiac arrhythmia susceptibility,
506 repolarization, and ion channels. *Curr Opin Pharmacol*. 2021;57:13-20. doi:
507 10.1016/j.coph.2020.09.015
508 43. Jeyaraj D, Haldar SM, Wan X, McCauley MD, Ripperger JA, Hu K, Lu Y, Eapen
509 BL, Sharma N, Ficker E, et al. Circadian rhythms govern cardiac repolarization
510 and arrhythmogenesis. *Nature*. 2012;483:96-99. doi: 10.1038/nature10852
511 44. D'Souza A, Wang Y, Anderson C, Bucchi A, Baruscotti M, Olieslagers S, Mesirca
512 P, Johnsen AB, Mastitskaya S, Ni H, et al. A circadian clock in the sinus node
513 mediates day-night rhythms in Hcn4 and heart rate. *Heart Rhythm*. 2021;18:801-
514 810. doi: 10.1016/j.hrthm.2020.11.026
515 45. Hayter EA, Wehrens SMT, Van Dongen HPA, Stangherlin A, Gaddameedhi S,
516 Crooks E, Barron NJ, Venetucci LA, Neill JSO, Brown TM, et al. Distinct
517 circadian mechanisms govern cardiac rhythms and susceptibility to arrhythmia.
518 *Nat Commun*. 2021;12:2472. doi: 10.1038/s41467-021-22788-8
519 46. Postema PG, Wilde AA. The measurement of the QT interval. *Curr Cardiol Rev*.
520 2014;10:287-294. doi: 10.2174/1573403x10666140514103612
521 47. Mitchell GF, Jeron A, Koren G. Measurement of heart rate and Q-T interval in the
522 conscious mouse. *Am J Physiol*. 1998;274:H747-751. doi:
523 10.1152/ajpheart.1998.274.3.H747
524 48. Roussel J, Champeroux P, Roy J, Richard S, Fauconnier J, Le Guennec JY,
525 Thireau J. The Complex QT/RR Relationship in Mice. *Sci Rep*. 2016;6:25388.
526 doi: 10.1038/srep25388
527 49. Refinetti R. Circadian rhythmicity of body temperature and metabolism.
528 *Temperature (Austin)*. 2020;7:321-362. doi: 10.1080/23328940.2020.1743605
529 50. Fleming PR, Muir FH. Electrocardiographic changes in induced hypothermia in
530 man. *Br Heart J*. 1957;19:59-66. doi: 10.1136/hrt.19.1.59
531 51. Hicks CE, McCord MC, Blount SG, Jr. Electrocardiographic changes during
532 hypothermia and circulatory occlusion. *Circulation*. 1956;13:21-28. doi:
533 10.1161/01.cir.13.1.21
534 52. Karjalainen J, Viitasalo M. Fever and cardiac rhythm. *Arch Intern Med*.
535 1986;146:1169-1171.
536 53. Mattu A, Brady WJ, Perron AD. Electrocardiographic manifestations of
537 hypothermia. *Am J Emerg Med*. 2002;20:314-326. doi: 10.1053/ajem.2002.32633
538 54. Yaganti VM, Naik CA, Dhond AJ. Electrocardiographic manifestations in a
539 hypothermic patient: review of Osborn waves. *Indian Heart J*. 2007;59:80-82.
540 55. Molnar J, Zhang F, Weiss J, Ehlert FA, Rosenthal JE. Diurnal pattern of QTc
541 interval: how long is prolonged? Possible relation to circadian triggers of

542 cardiovascular events. *J Am Coll Cardiol*. 1996;27:76-83. doi: 10.1016/0735-
543 1097(95)00426-2
544 56. Browne KF, Prystowsky E, Heger JJ, Chilson DA, Zipes DP. Prolongation of the
545 Q-T interval in man during sleep. *Am J Cardiol*. 1983;52:55-59. doi:
546 10.1016/0002-9149(83)90068-1
547 57. Sabir IN, Killeen MJ, Grace AA, Huang CL. Ventricular arrhythmogenesis:
548 insights from murine models. *Prog Biophys Mol Biol*. 2008;98:208-218. doi:
549 10.1016/j.pbiomolbio.2008.10.011
550
551

552 **Figure Legends**
553
554 **Figure 1. L-RF causes a simultaneous shift in the daily rhythms of the RR, QT,**
555 **and PR intervals, Tb, and strength of the pHF component. A.** Representative hourly
556 averaged ECG traces recorded from a mouse in ALF (left), after initially starting L-RF
557 (middle), or 2 weeks after starting L-RF (right). **B.** Averaged time series (n = 6 mice,
558 data points are averaged data and SD) data showing 3 consecutive days of the hourly
559 mean for the RR interval (vermillion), QT interval (sky blue), PR interval (orange), Tb
560 (reddish purple), pHF (blue), and activity (yellow). The data are plotted as a function of
561 ZT and the shaded regions correspond to the dark cycle. Left column shows the data
562 recorded during ALF, middle column shows the data recorded initially after starting L-RF
563 (boxed arrow indicates 24 hours after the start of L-RF), and right column shows the
564 data recorded 2 weeks after starting L-RF. The solid lines shown for the time series
565 ECG and Tb data in ALF, 24 hours after the start of L-RF, and 2 weeks after the start of
566 L-RF are cosine curve fit to the averaged data.
567
568 **Figure 2. L-RF causes a simultaneous shift and increased amplitude in the 24-**
569 **hour rhythms of the mean RR, QT, and PR intervals and Tb.** The individual mouse
570 time series data for the RR, QT, and PR intervals, and Tb were fit to a cosine wave to
571 calculate the acrophase, period, mesor, and amplitude for mice in ALF, 24 hours after
572 initially starting L-RF ($L\text{-}RF_i$), and 2 weeks after starting L-RF ($L\text{-}RF_{2wk}$). **A.** The top row
573 shows the acrophase of the RR interval (vermillion), QT interval (sky blue), PR interval
574 (orange), and Tb (reddish purple) for each condition. The second row, left graph, shows
575 the difference in the acrophase of the RR interval, QT interval, PR interval, and Tb
576 measured from mice in ALF compared to those from mice 24 hours after initially starting
577 L-RF or 2 weeks after starting L-RF. The second row, right graph, shows the period of
578 the RR interval, QT interval, PR interval, and Tb from mice in ALF, 24 hours after
579 initially starting L-RF, and 2 weeks after starting L-RF. **B.** The top row shows the mesor
580 and second row shows the amplitude of the RR interval, QT interval, PR interval, and
581 Tb for each condition (n = 6 mice per group, *p<0.05, **p<0.01, ***p<0.001,
582 ****p<0.0001. The horizontal bar in each data set is the mean).
583
584 **Figure 3. Cross-correlation analysis between the RR interval and Tb or strength of**
585 **the pHF component before and after L-RF shows correlated and aligned**
586 **rhythmicity.** The average of the cross-correlation between the time series data for the
587 RR interval and Tb (top row, reddish purple), pHF component (middle row, blue), and
588 activity (bottom row, yellow) in ALF (left column), 24 hours after initially starting L-RF
589 (middle column), and 2 weeks after starting L-RF (right column). The peak correlation
590 coefficient at lag 0 is shown (n = 6 mice per group, data points are mean data and SD,
591 *p<0.05 and **p<0.01).
592
593 **Figure 4. Propranolol and atropine prevent the daily rhythms in RR interval and**
594 **Tb in mice during L-RF. A.** Time series data showing the hourly mean in the RR
595 interval (vermillion) and Tb (reddish purple) recorded 1 week after the start of L-RF (ZT
596 3 to ZT 9). The data are plotted as a function of ZT and the shaded regions represent
597 the dark cycle. The time series shows the average of the hourly mean data and SD

measured during the light and dark cycle the day before starting the propranolol and atropine injections (LC0, DC0), and the first and second light and dark cycles after injecting mice at ZT 23.5 and ZT 9.5 (LC1, DC1, LC2, and DC2, respectively, injection times are denoted by arrows; n = 5 mice). **B.** Shown are the 24-hour means in the pHF (sky blue) and pLF (blue) components measured from the mice during the four before and after the first propranolol and atropine injections (horizontal bar in each data set is the mean, *p<0.05). **C.** Shown are the mean RR interval (vermillion) and Tb (reddish purple) data recorded during the light and dark cycle on day before (LC0 and DC0) or the days after starting the injections with propranolol and atropine (LC1, DC1, LC2 and DC2; horizontal bar in each data set is the mean, *p<0.05; ***p<0.001).

Figure 5. Correcting the QT-interval for Tb causes a loss in the daily rhythm in the QT interval. A. Left graph shows the hourly mean in the QT interval plotted as a function of the corresponding Tb for each mouse in ALF, initially after starting L-RF, or 2 weeks after starting L-RF (each mouse is represented by a different color, n = 6). The right graph shows the QT_{37^oC} interval is plotted as a function of the corresponding Tb for the same set of mice. Linear regression of the data for each mouse (red lines) were used to calculate the average slope and R^2 and SD for both the left and right graphs. **B.** Averaged time series for the hourly mean QT_{37^oC} interval and SD (sky blue) in ALF, initially after starting L-RF, and 2 weeks after the start of L-RF. Also shown is the corresponding averaged time series data for the hourly mean in the uncorrected QT interval data from **Figure 1** for direct comparison (grey). Data are plotted as a function of ZT and the shaded regions represent the dark cycle.

Figure 6. L-RF impacts the daily rhythms of the RR, QT, and PR intervals and Tb in *Scn5a*$^{+/\Delta KPQ}$ mice. A. Representative of hourly averaged ECG traces recorded from WT or *Scn5a*$^{+/\Delta KPQ}$ mice in ALF (left), after initially starting L-RF (middle), or 2 weeks after starting L-RF (right) at different ZT. The top row shows the times of day that the QT intervals were longest, and the bottom row corresponds to times of day when the QT intervals were shortest. **B.** Averaged time series (n = 6 mice, data points are mean data and SD) data showing 3 consecutive days of the hourly mean for the RR interval (vermillion), QT interval (sky blue), PR interval (orange), Tb (reddish purple), and the QT_{37^oC} interval (blue). The data are plotted as a function of ZT and the shaded regions correspond to the dark cycle. The time series for the QT_{37^oC} interval also includes the QT_{37^oC} interval measured from WT mice (grey) for direct comparison. Left column shows the data recorded during ALF, middle column shows the data recorded initially after starting L-RF (boxed arrow indicates 24 hours after the start of L-RF), and right column shows the data recorded 2 weeks after starting L-RF. The solid lines shown for the time series ECG and Tb data in ALF, 24 hours after the start of L-RF, and 2 weeks after the start of L-RF are cosine curve fit to the averaged data.

641 **Supplemental Material**
642
643 **Supplemental Figure Legends**
644
645 **Figure 1S. L-RF initially causes a decrease in mass, but the mice regain and**
646 **increase mass after 1 week in L-RF.** The left graphs shows the daily body mass of
647 mice of mice in ALF (yellow) or after initially starting L-RF (blueish green, n = 5 mice per
648 group, **p<0.01 ***p<0.001); the middle graph shows the average weekly mass in mice
649 during the first 2 weeks of L-RF (n = 6, *p<0.05 and **p<0.01); and the right graph
650 shows the average food consumption per mouse/day during each day after the start of
651 L-RF for 2 weeks (n=6).
652
653 **Figure 2S. Injecting L-RF mice with propranolol and atropine has little impact on**
654 **mean RR or Tb interval 2 hours after the injection.** The graphs show the 15 min
655 mean in the **A.** RR interval or **B.** Tb. The left panel of each graph shows the data on the
656 day before the injection (blue), and the right panel of each graph shows the data
657 immediately before and after injection (vermillion). The injection time is denoted by an
658 arrow labeled P+A. The left graphs in **A.** and **B.** show the data corresponding to the
659 transition of the dark (shaded) to light cycle on the day before the injection (LC0) or the
660 light cycle after the injection (LC1). The injection time was ZT 23.5. The right graphs in
661 **A.** and **B.** show the data corresponding to light cycle on the day before the injection
662 (LC0) or the light cycle after the injection (LC1). The injection time was ZT 9.5. (n = 5,
663 *p<0.05).
664
665 **Figure 3S. L-RF causes genotype specific differences in the 24-hour rhythms of**
666 **the mean RR, QT, and PR intervals and Tb measured from WT and *Scn5a*$^{+/\Delta KPQ}$**
667 **mice. A.** The individual mouse time series data for the RR, QT, and PR intervals, and
668 Tb were fit to a cosine wave to calculate the mesor and amplitude for *Scn5a*$^{+/\Delta KPQ}$ mice
669 in ALF, 24 hours after initially starting L-RF (L-RF$_i$), and 2 weeks after starting L-RF (L-
670 RF$_{2wk}$). The top row shows the mesor and second row shows the amplitude of the RR
671 interval (vermillion), QT interval (sky blue), PR interval (orange), and Tb (reddish purple)
672 measured from *Scn5a*$^{+/\Delta KPQ}$ mice for each condition. The horizontal bar in each data set
673 is the mean. Also included are the corresponding WT data presented in Figure 2 (grey)
674 for comparison (n = 6 mice per group, *p<0.05, **p<0.01, ***p<0.001, ****p<0.0001). **B.**
675 The graph shows the average of the mean QT$_{37^oC}$ interval measured from WT (grey) or
676 *Scn5a*$^{+/\Delta KPQ}$ mice (blue) in ALF, one day after starting L-RF, and two weeks after
677 starting L-RF. The horizontal bar in each data set is the mean (n = 6, *p<0.05).
678
679 **Figure 4S. L-RF does not cause torpor.** Shown are the Tb profiles for each individual
680 WT mice in ALF, 24 hours after initially starting L-RF (L-RF$_i$), and 2 weeks after starting
681 L-RF (L-RF$_{2wk}$). Only one mouse showed a transient decrease in the Tb < 33°C
682 (asterisk).
683
684 **Figure 5S. L-RF does not alter HR after injection with propranolol and atropine.**
685 We injected mice in ALF (yellow) or after two weeks of L-RF (bluish green) and
686 recorded the mean RR interval using ECGenie (Mouse Specifics, Inc., Boston, MA,

687 USA). The data were collected between ZT 0.5-3. The ECGenie system comprises a
688 platform with electrodes connected to an amplifier (e-MOUSE) that measures ECG non-
689 invasively. The mice were injected with propranolol and atropine (P+A) 15 minutes prior
690 to recording the ECGs (n = 4 mice per group, the horizontal bar in each data set is the
691 mean).

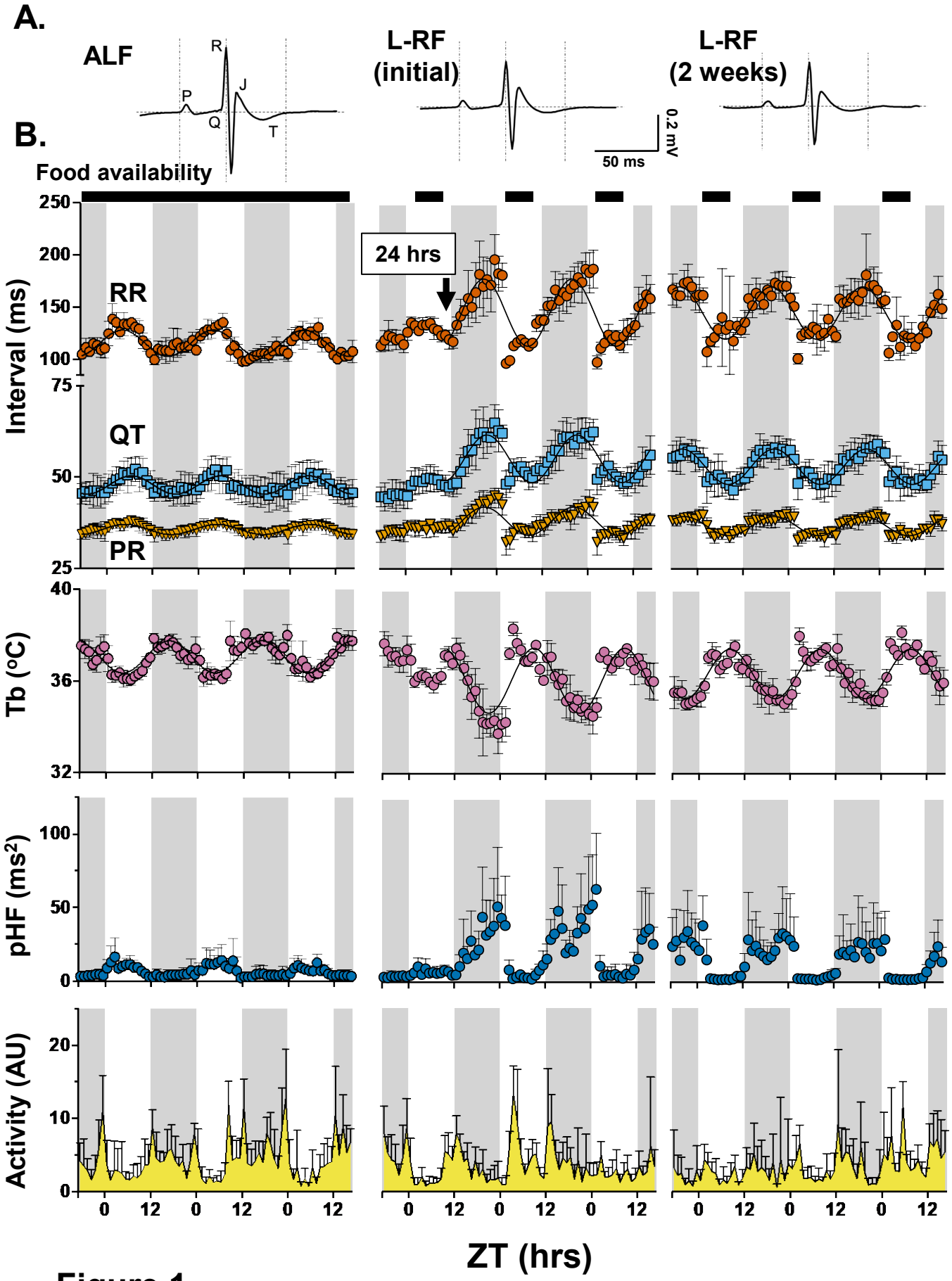
A.
ALF
R
J
P
Q
T
L-RF
(initial)
L-RF
(2 weeks)
0.2 mV
50 ms
B.
Food availability
24 hrs
RR
QT
PR
Interval (ms)
Tb (°C)
pHF (ms²)
Activity (AU)
ZT (hrs)

Figure 1.

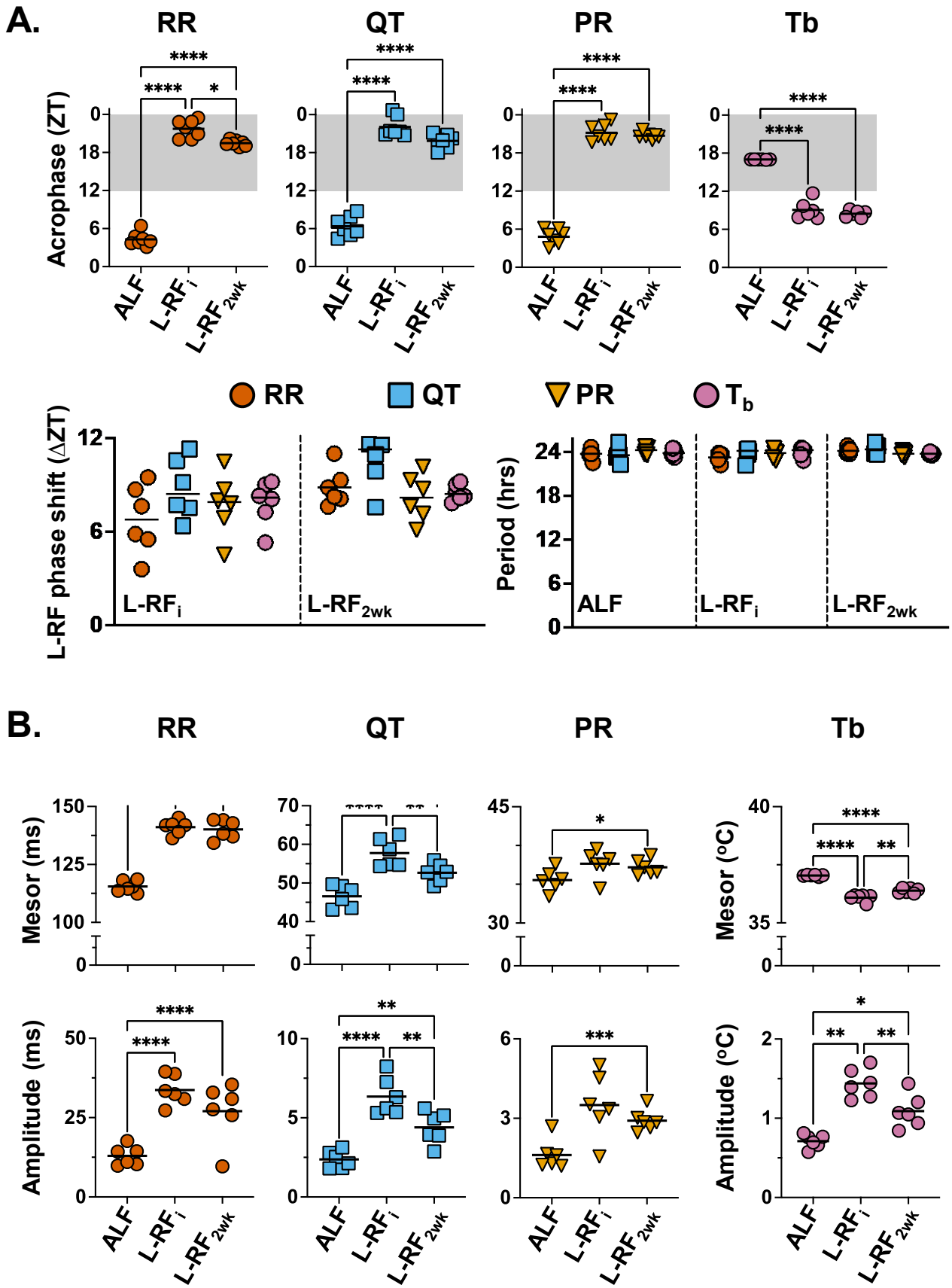
A.
RR
QT
PR
Tb
Acrophase (ZT)
ALF
L-RF$_i$
L-RF$_{2wk}$
RR
QT
PR
T$_b$
L-RF phase shift (ΔZT)
L-RF$_i$
L-RF$_{2wk}$
Period (hrs)
ALF
L-RF$_i$
L-RF$_{2wk}$
B.
RR
QT
PR
Tb
Mesor (ms)
Mesor (°C)
Amplitude (ms)
Amplitude (°C)
ALF
L-RF$_i$
L-RF$_{2wk}$

Figure 2.

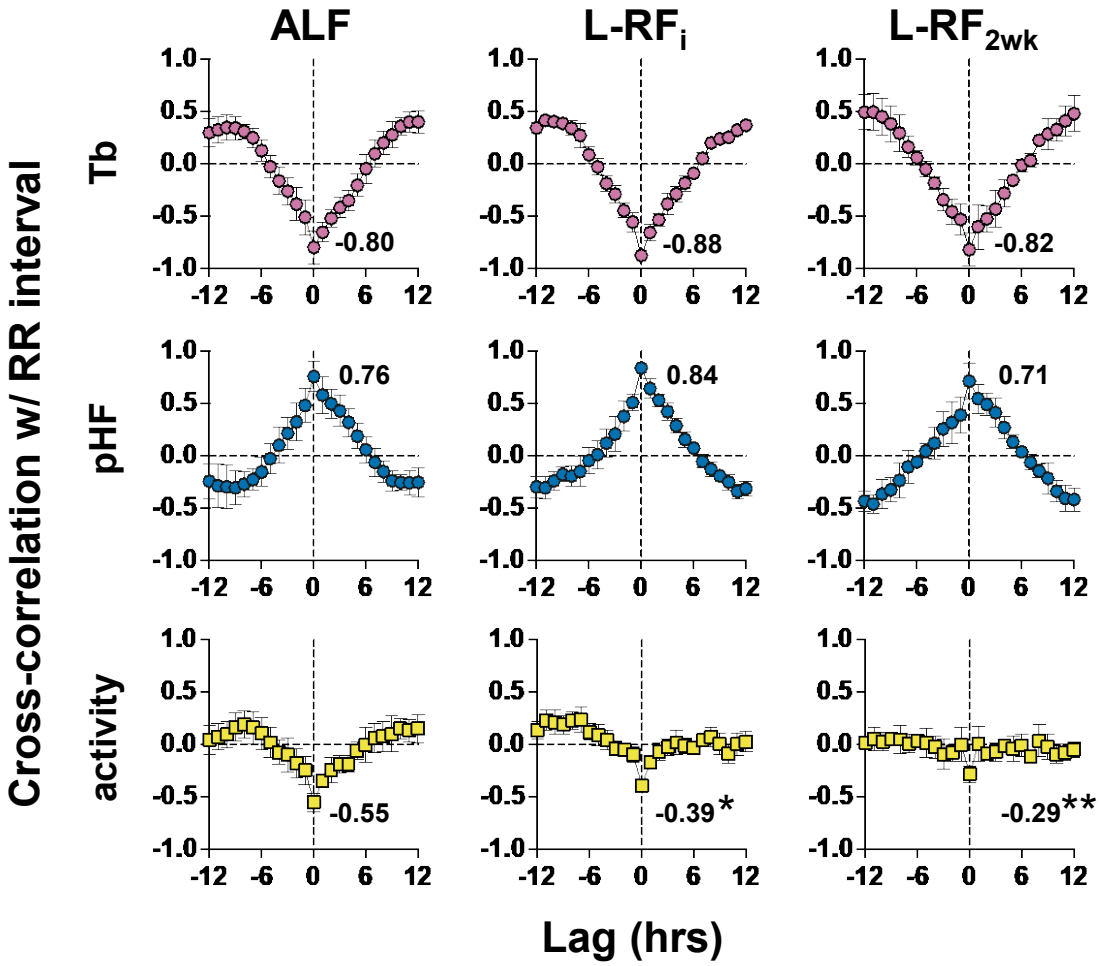
ALF
L-RF$_i$
L-RF$_{2wk}$
Tb
pHF
activity
Cross-correlation w/ RR interval
Lag (hrs)
-0.80
-0.88
-0.82
0.76
0.84
0.71
-0.55
-0.39*
-0.29**

Figure 3.

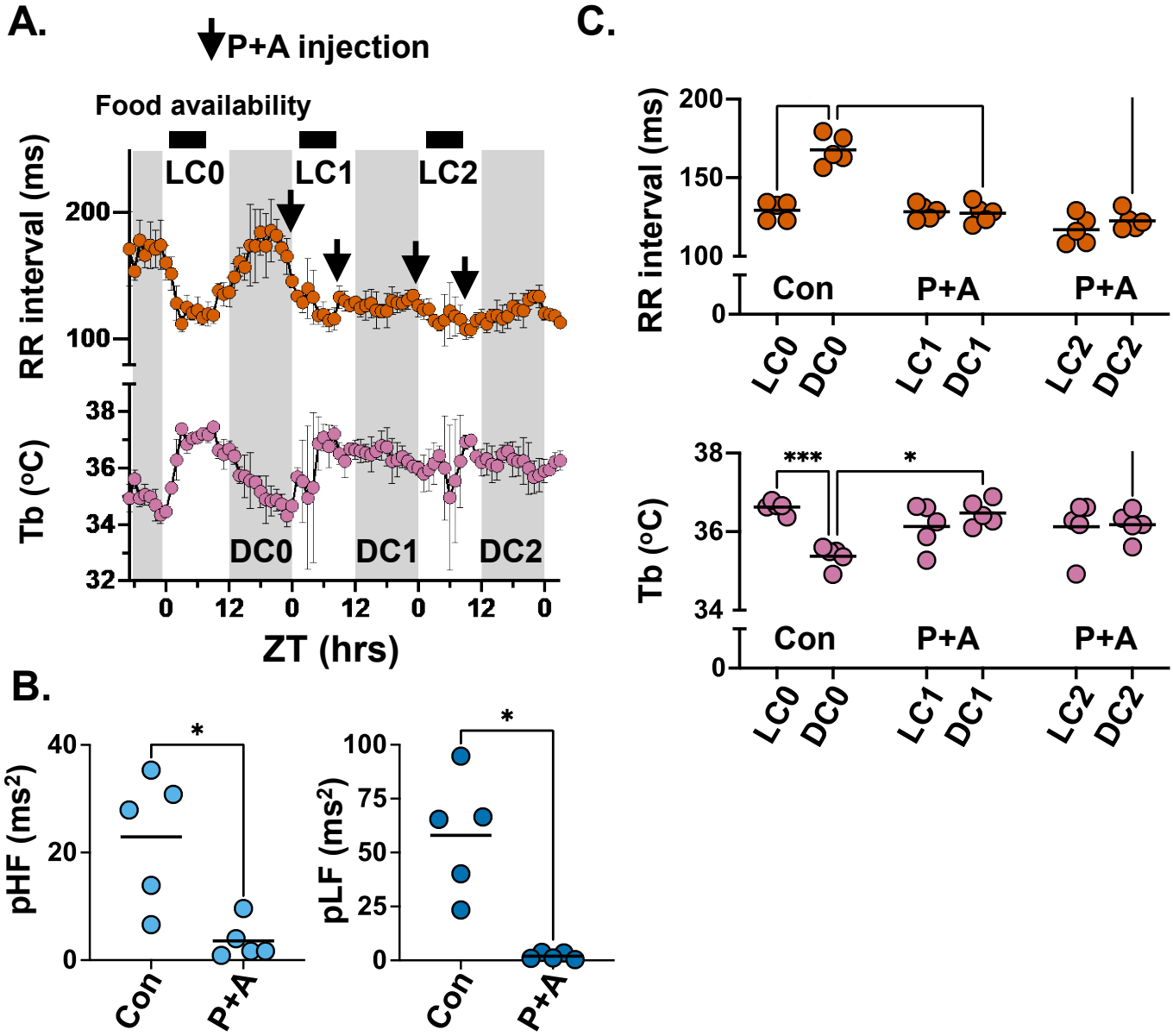
A.
P+A injection
Food availability
LC0
LC1
LC2
RR interval (ms)
200
100
Tb (°C)
38
36
34
32
DC0
DC1
DC2
0
12
0
12
0
12
0
ZT (hrs)
B.
pHF (ms²)
40
20
0
*
Con
P+A
pLF (ms²)
100
75
50
25
0
*
Con
P+A
C.
RR interval (ms)
200
150
100
0
Con
P+A
P+A
LC0
DC0
LC1
DC1
LC2
DC2
Tb (°C)
38
36
34
0
***
*
Con
P+A
P+A
LC0
DC0
LC1
DC1
LC2
DC2

Figure 4.

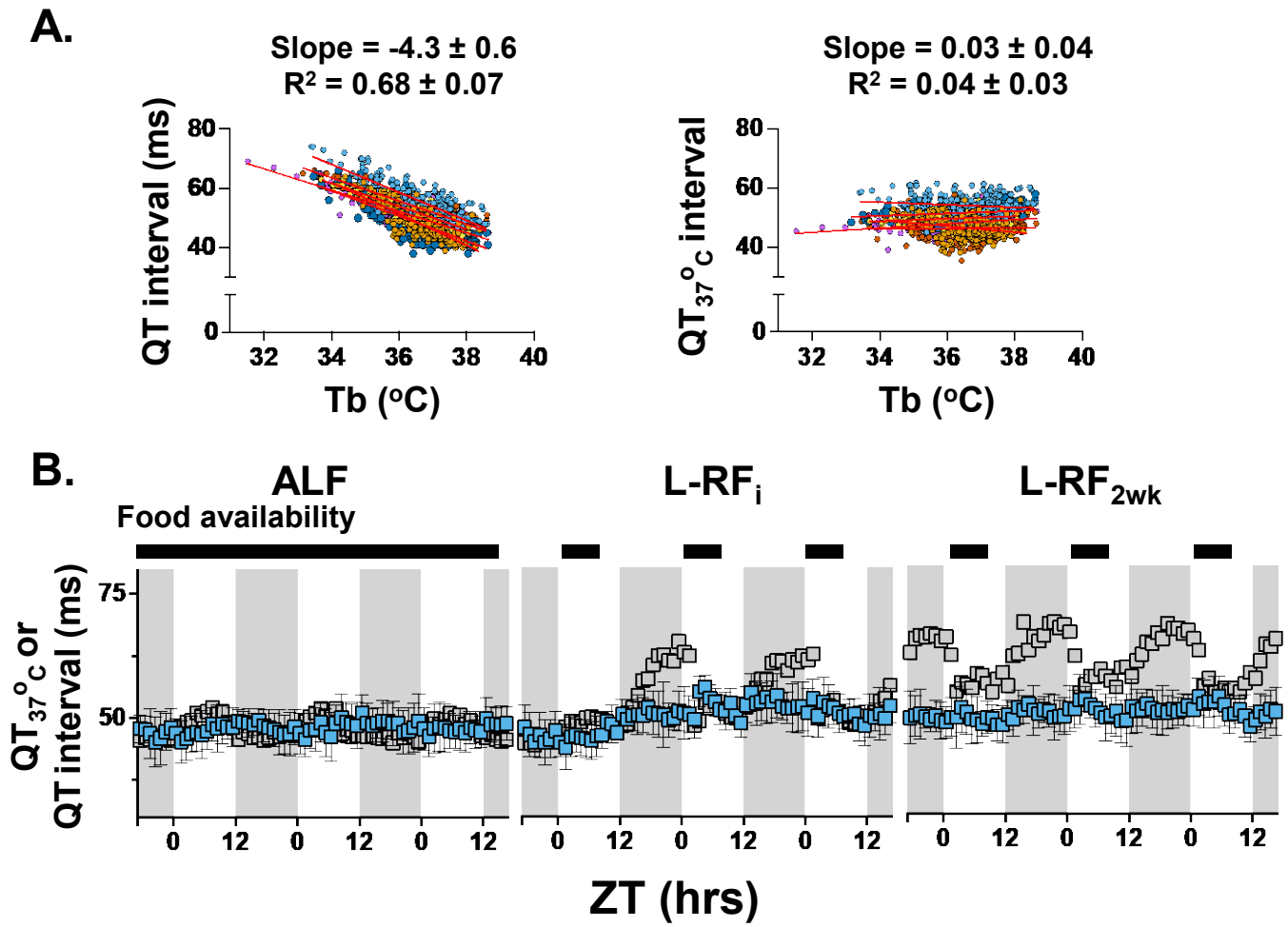
A.
Slope = -4.3 ± 0.6
R² = 0.68 ± 0.07
QT interval (ms)
Tb (°C)
Slope = 0.03 ± 0.04
R² = 0.04 ± 0.03
QT37°C interval
Tb (°C)
B.
ALF
L-RFi
L-RF2wk
Food availability
QT37°C or QT interval (ms)
ZT (hrs)

Figure 5.

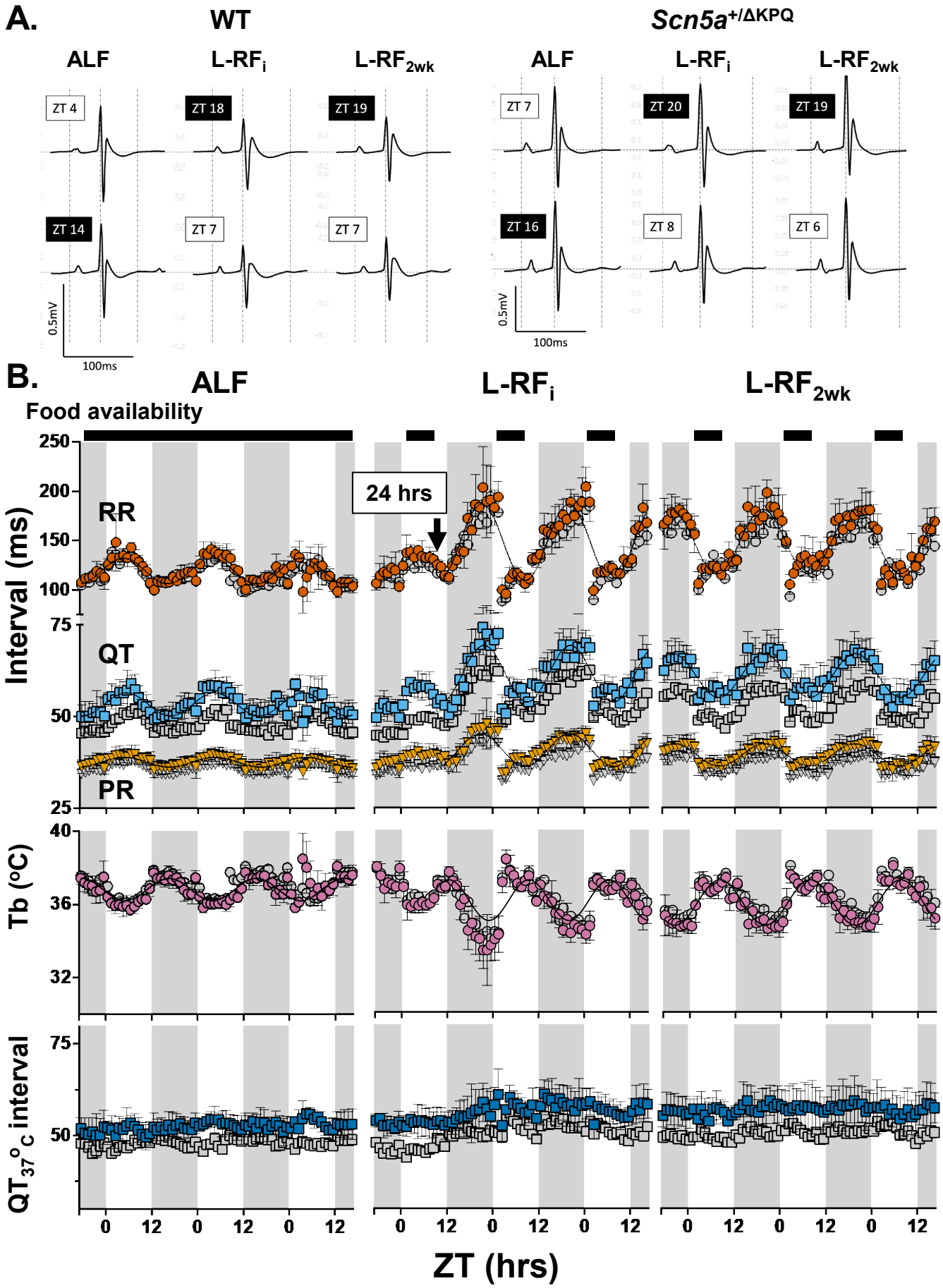
A.
WT
Scn5a+/ΔKPQ
ALF
L-RFi
L-RF2wk
ALF
L-RFi
L-RF2wk
ZT 4
ZT 18
ZT 19
ZT 7
ZT 20
ZT 19
ZT 14
ZT 7
ZT 7
ZT 16
ZT 8
ZT 6
0.5mV
100ms
0.5mV
100ms
B.
ALF
L-RFi
L-RF2wk
Food availability
24 hrs
RR
QT
PR
Interval (ms)
Tb (°C)
QT37°C interval
ZT (hrs)

Figure 6.

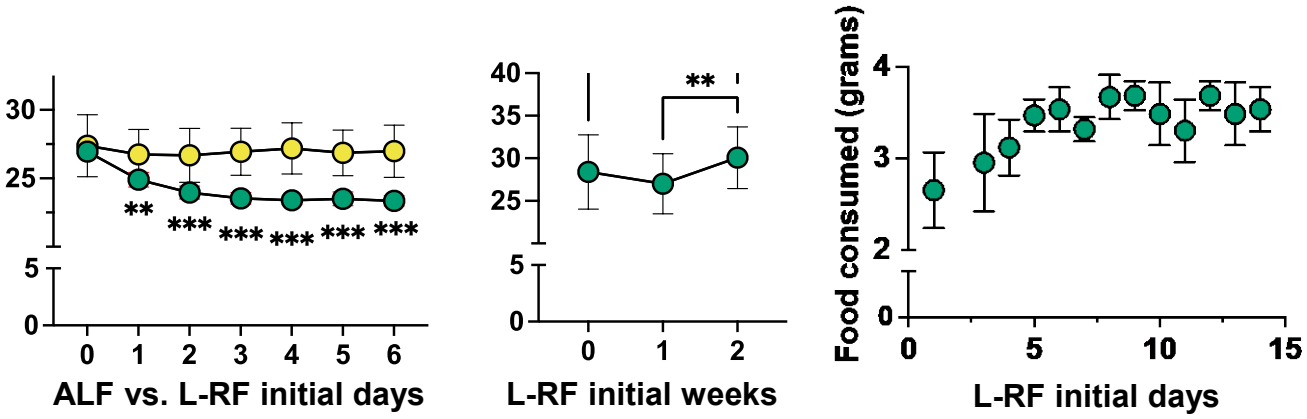

Supplement Figure 1.

A.

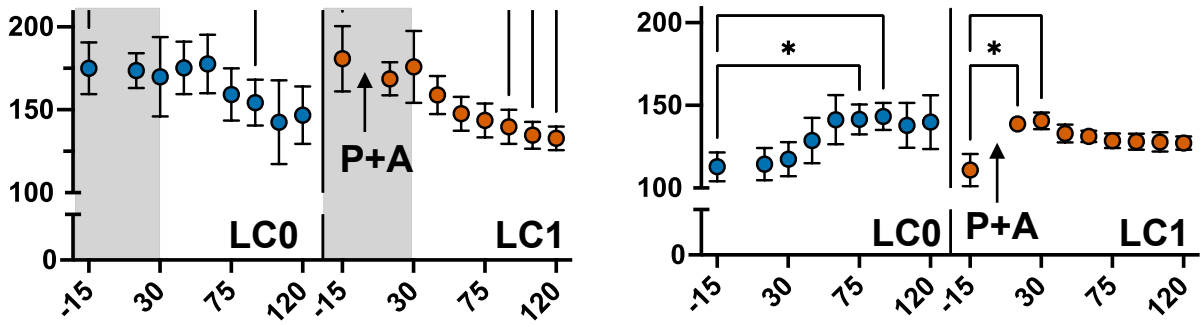

B.

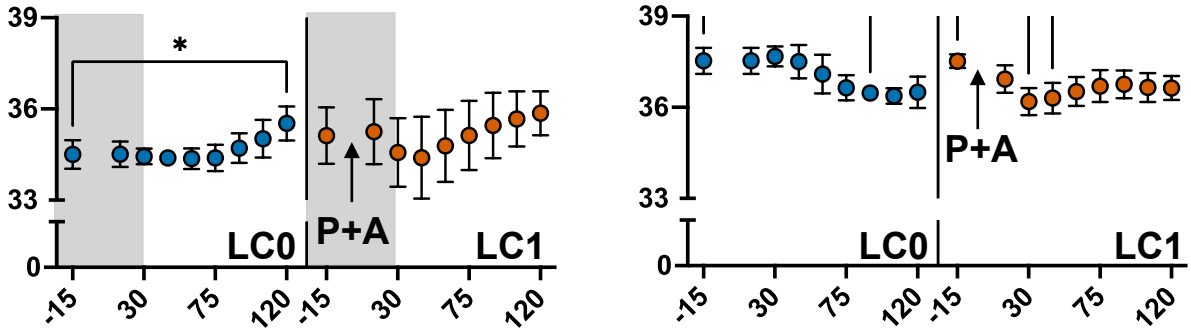

Supplement Figure 2.

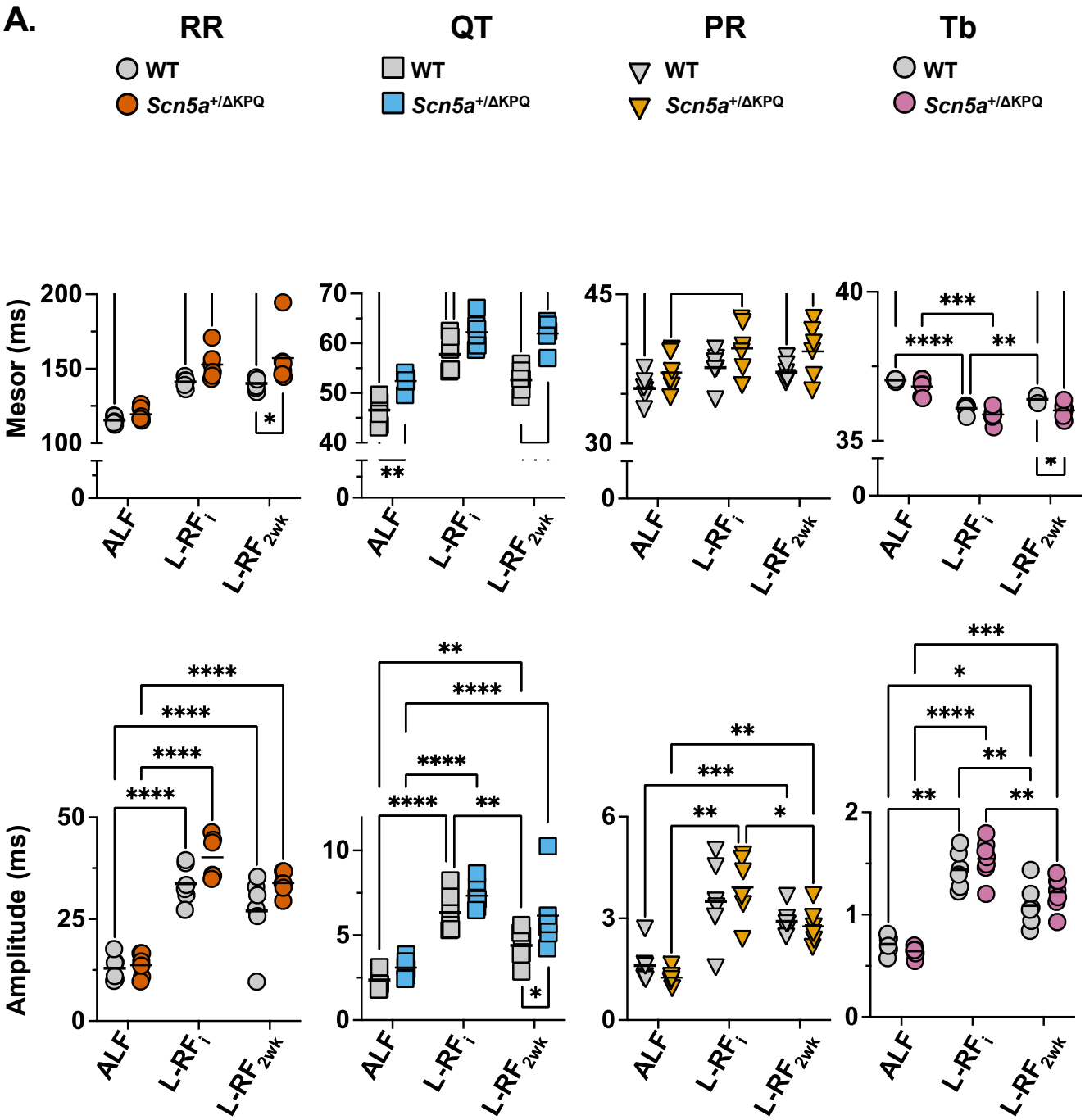

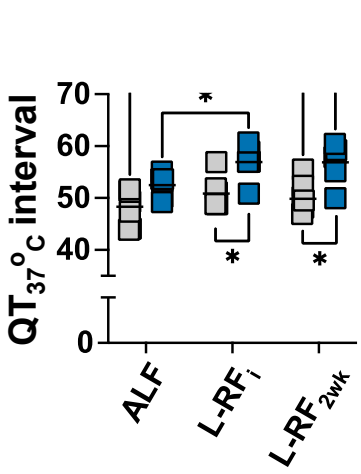

Supplement Figure 3.

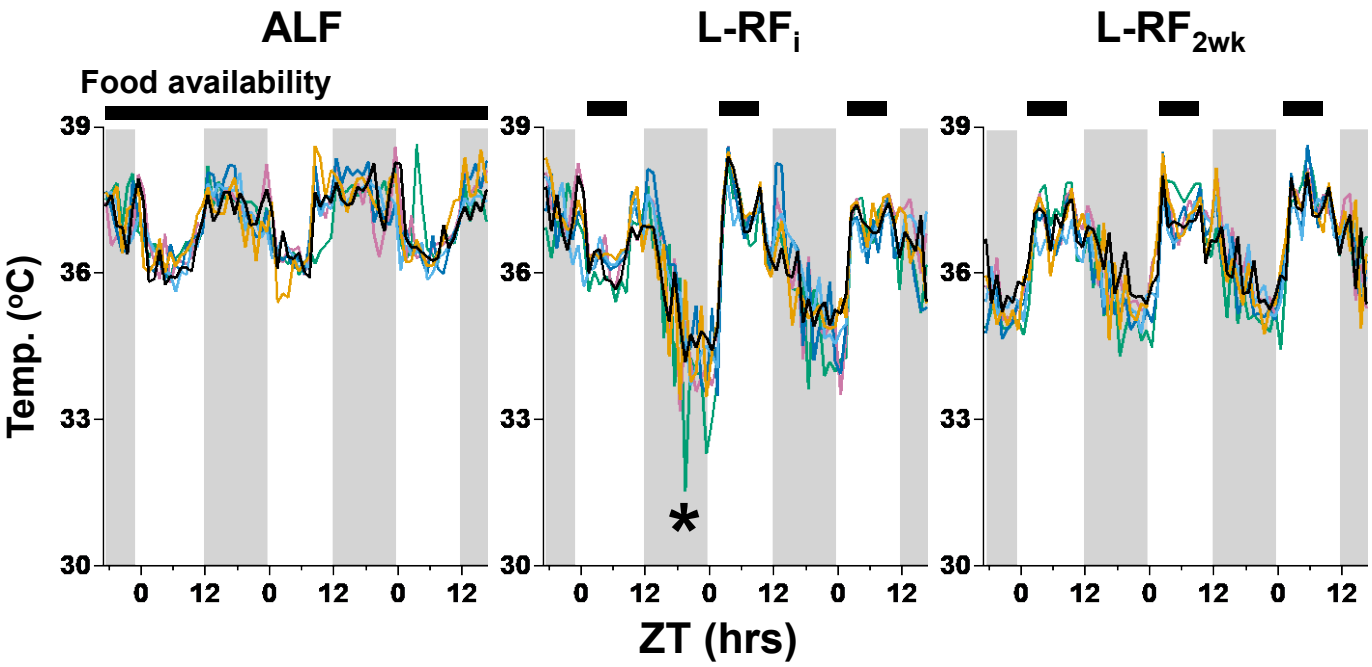

Supplement Figure 4.

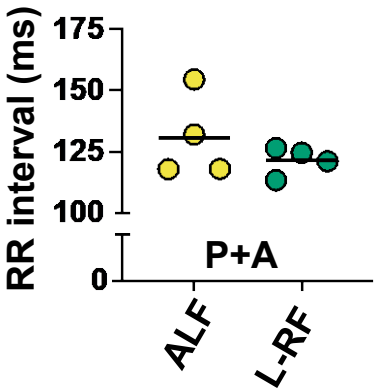

Supplement Figure 5.